

Dynamics and Stability of Acoustic Wavefronts in the Ocean

Oleg A. Godin

CIRES/Univ. of Colorado and NOAA/Earth System Research Lab., Physical Sciences Division,
R/PSD99, 325 Broadway
Boulder, CO 80305-3328

phone: (303) 497-6558 fax: (303) 497-5862 email: oleg.godin@noaa.gov

Award Number: N00014-08-1-0100

<http://cires.colorado.edu>

LONG-TERM GOALS

- To develop a method of modeling sound propagation in an environment with multi-scale inhomogeneities, which preserves the efficiency and intuitive qualities of the ray theory but is free from spurious environmental sensitivity and strong perturbations associated with ray trajectories.
- To investigate and quantify effects on underwater acoustic wavefronts of internal gravity waves, sea swell, “spice,” and other small-scale processes in the water column.

OBJECTIVES

1. To assess significance of time dependence of the sound speed and flow velocity perturbations on predictability of acoustic wavefronts and timefronts.
2. To quantify horizontal refraction of sound by random meso-scale inhomogeneities at $O(1)$ Mm propagation ranges.
3. To find the variance and bias of random ray travel times in the regime, where the ray displacement may be comparable to the vertical extent of the underwater waveguide but the clustering has not developed yet.
4. To determine, using a perturbation theory and numerical simulations, typical propagation ranges where clustering of chaotic rays replaces the anisotropy of ray scattering as the main physical mechanism responsible for acoustic wavefront stability.
5. To develop an efficient technique for modeling acoustic wavefronts and their perturbations in range-dependent and horizontally inhomogeneous oceans.
6. To model perturbations of acoustic wavefronts and timefronts by internal gravity waves, internal tides, sea swell, and “spice” in the ocean.
7. To investigate implications of wavefront stability on the downward extension of acoustic timefronts and deepening of lower turning points of steep rays due to small- and meso-scale physical processes in the upper ocean.

Report Documentation Page

Form Approved
OMB No. 0704-0188

Public reporting burden for the collection of information is estimated to average 1 hour per response, including the time for reviewing instructions, searching existing data sources, gathering and maintaining the data needed, and completing and reviewing the collection of information. Send comments regarding this burden estimate or any other aspect of this collection of information, including suggestions for reducing this burden, to Washington Headquarters Services, Directorate for Information Operations and Reports, 1215 Jefferson Davis Highway, Suite 1204, Arlington VA 22202-4302. Respondents should be aware that notwithstanding any other provision of law, no person shall be subject to a penalty for failing to comply with a collection of information if it does not display a currently valid OMB control number.

1. REPORT DATE 30 SEP 2014		2. REPORT TYPE		3. DATES COVERED 00-00-2014 to 00-00-2014	
4. TITLE AND SUBTITLE Dynamics and Stability of Acoustic Wavefronts in the Ocean				5a. CONTRACT NUMBER	
				5b. GRANT NUMBER	
				5c. PROGRAM ELEMENT NUMBER	
6. AUTHOR(S)				5d. PROJECT NUMBER	
				5e. TASK NUMBER	
				5f. WORK UNIT NUMBER	
7. PERFORMING ORGANIZATION NAME(S) AND ADDRESS(ES) University of Colorado, 325 Broadway, Boulder, CO, 80305				8. PERFORMING ORGANIZATION REPORT NUMBER	
9. SPONSORING/MONITORING AGENCY NAME(S) AND ADDRESS(ES)				10. SPONSOR/MONITOR'S ACRONYM(S)	
				11. SPONSOR/MONITOR'S REPORT NUMBER(S)	
12. DISTRIBUTION/AVAILABILITY STATEMENT Approved for public release; distribution unlimited					
13. SUPPLEMENTARY NOTES					
14. ABSTRACT					
15. SUBJECT TERMS					
16. SECURITY CLASSIFICATION OF:			17. LIMITATION OF ABSTRACT Same as Report (SAR)	18. NUMBER OF PAGES 9	19a. NAME OF RESPONSIBLE PERSON
a. REPORT unclassified	b. ABSTRACT unclassified	c. THIS PAGE unclassified			

APPROACH

Our primary theoretical approach is an extension of the method employed in (Godin, 2003, 2007, 2009), where a novel perturbation technique has been developed to solve the eikonal equation and calculate wavefront and ray trajectory displacements, which are required to be small over a correlation length of the environmental inhomogeneities but not necessarily over the entire acoustic propagation path. Methods based on the geometrical acoustics have been supplemented by full-wave approaches (Brekhovskikh and Godin, 1999), including a normal-mode theory for range-dependent and horizontally inhomogeneous waveguides.

The analytical methods have been complemented by numerical wavefront-tracing techniques. A major problem with a direct modeling of acoustic wavefronts in the ocean through numerical solution of the eikonal equation lies in the eikonal (and acoustic travel time) being a multi-valued function of position. A number of computational approaches to solve the eikonal equation without ray tracing had been developed in mathematical and seismological communities (Vidale, 1990; Sava and Fomel, 2001; Sethian, 2001, Benamou, 2003). However, most of these methods are only capable of tracing the wavefront of the earliest, first arrival and thus are not suitable for underwater acoustic applications. We have adapted to ocean acoustics problems the Lagrangian wavefront construction techniques (Vinje et al., 1993, 1999; Lambaré et al., 1996; Sava and Fomel, 2001; Chambers and Kendall, 2008; Hauser et al., 2008), which were originally developed in the context of exploration seismology and are capable of computing all arrivals. Extension of the existing wavefront construction techniques to long-range underwater sound propagation is a non-trivial and, in fact, rather challenging task because the number of ray arrivals and topological complexity of wavefronts in the ocean far exceed those in the geophysical applications considered to date.

Theoretical results and new modeling capabilities have been verified against numerical simulations performed with well-established ray and PE propagation codes.

The key individuals that have been involved in this work are Oleg A. Godin (CIRES/Univ. of Colorado and NOAA/ESRL), Nikolay A. Zabolin (CIRES/Univ. of Colorado), and L. Y. Zabolina (ECEE/Univ. of Colorado). Dr. Zabolin and Ms. Zabolina focused on developing and testing an efficient computer code for modeling acoustic wavefronts in inhomogeneous, moving fluids. Dr. Godin took the lead in theoretical description of effects of the ocean currents, localized inhomogeneities, and sound-speed time-dependence on the acoustic wavefronts.

WORK COMPLETED

Most of the work on the project was completed by the end of FY'13. In FY'14, our 3-D Huygens Wavefront Tracing (3-D HWT) algorithm was applied to study effects of various oceanographic processes on underwater acoustic fields. The 3-D HWT algorithm was also applied to investigate long-range propagation of infrasound in the atmosphere (Zabolin et al., 2014) and of infragravity waves in the ocean (Godin et al., 2014). Infragravity waves are surface gravity waves with periods from ~0.5 to ~50 minutes. Infragravity waves are refracted by ocean currents and, especially, by seafloor bathymetry and can be treated in horizontally inhomogeneous ocean using the vertical modes – horizontal rays theory [see, e.g., (Brekhovskikh and Godin, 1999)]. The 3-D HWT algorithm was used

to simulate horizontal structure of infragravity wave fields and interpret observations of seafloor pressure fluctuations (Godin et al., 2014).

RESULTS

A software package was developed for numerical modeling of 3-D sound propagation in the ocean, where sound speed and current velocity are arbitrary smooth functions of three spatial coordinates. The package is freely available through the Ocean Acoustics Library at http://oalib.hlsresearch.com/Rays/HWT_3D_mm_v.1.0/. The software package is a numerical implementation of an alternative formulation of the geometrical acoustics, where wavefronts rather than rays are the geometric “backbone” of the wave field. Wavefront tracing can be viewed as a direct implementation of the Huygens’ principle. Our current wavefront tracing algorithm (Zabotin et al., 2014) is an extension to three-dimensionally inhomogeneous, moving media of an earlier 2-D algorithm for sound in moving fluids (Zabotin et al., 2012) and the original Huygens Wavefront Tracing (HWT) algorithm (Sava and Fomel, 2001), developed as a part of the open-source Madagascar project for seismic modeling and imaging. Aside from generalization to moving media, the extended HWT algorithm improves the accuracy and stability of the original algorithm and includes new functionality to account for sound reflections at sloping boundaries and to efficiently model acoustic timefronts in addition to the wavefronts. For wavefront tracing in inhomogeneous media, HWT is much more computationally efficient and robust than traditional ray codes (Sava and Fomel, 2001). Unlike many other eikonal solvers, the HWT method produces the output in ray coordinates and has the important ability to track multiple arrivals. With the HWT method, each wavefront is generated from the preceding one by finite differences in the ray-coordinates domain.

The 3-D HWT algorithm has been applied to study effects of various oceanographic processes on underwater sound propagation and also has been demonstrated to be an efficient and robust technique for modeling infrasound propagation in the atmosphere (Zabotin et al., 2014).

To illustrate application of the 3-D wavefront tracing to modeling sound propagation in shallow water, we consider environmental conditions similar to that of the 1995 Shallow-Water Acoustic Random Media (SWARM) experiment (Apel et al., 1997). Rather strong sound speed variations in time and in the horizontal plane were encountered during the SWARM experiment. The sound-speed variability was primarily due to packets of nonlinear internal gravity waves (IW), which were generated by tides on a shelfbreak. We follow (Apel, 2003; Godin et al., 2006) and use the “dnoidal” model of the vertical isopycnal displacement in the nonlinear IW packets. In our simulations we placed the source of sound at the point with coordinates $x = 0$, $y = 5000$ m, $z = 20$ m. The source depth corresponds to the peak of the first IW mode shape function. Distortions of a particular wavefront, which corresponds to the acoustic travel time of 6 s, are shown in Figure 1 for different positions, i.e., stages of evolution, of the IW packet. The IW packet positions are characterized by distance $D = Vt$ the packet covered since its generation; $D = 0$ corresponds to sound propagation in the absence of IWs, while $D = 30$ km corresponds to the time, when the peak of the sound speed distortion reaches the $y = 5000$ m plane. Note that the acoustic wavefront maintains its general shape during the IW packet propagation despite strong perturbations of individual rays (not shown) that form the wavefront.

Relative variations of sound speed in the atmosphere are much larger than in the ocean. Unlike the ocean, where the Mach number of currents, understood as the ratio of the flow velocity to the sound

speed, rarely exceeds 10^{-3} , winds can have Mach numbers as large as 0.5 and are a major factor shaping acoustic fields. Combined with strong variations of the sound speed and wind velocity with height, this leads to a rather complicated arrival structure of acoustic fields due to distant compact sources. Understanding and utilizing acoustic arrivals in the atmosphere requires an accurate modeling of sound propagation in moving fluids. We illustrate atmospheric applications of the HWT algorithm by modeling propagation of infrasound generated by Eyjafjallajökull volcano in southern Iceland. Eruptions of this volcano were recorded by infrasonic sensors at distances up to 3700 km in 2010 (Drob et al., 2010).

Modern atmospheric models, such as the Whole Atmosphere Community Climate Model (WAM) (Liu et al., 2010; Akmaev, 2011), provide information about three-dimensional distributions of all major atmospheric parameters necessary for sound-speed calculations: the temperature T , zonal (u) and meridional (v) components of the wind velocity as well as the content of water vapor and other chemical constituents. To specify the propagation medium, we used a version of WAM output that provides ~ 2 deg resolution in geographic coordinates and 150 unevenly distributed grid points in the altitude, from 0 to 500 km above sea level (Figure 2). Figures 2b, c illustrates the complicated spatial structure of the horizontal and vertical variations of the physical parameters of the atmosphere that govern infrasound propagation in the Eyjafjallajökull volcano vicinity.

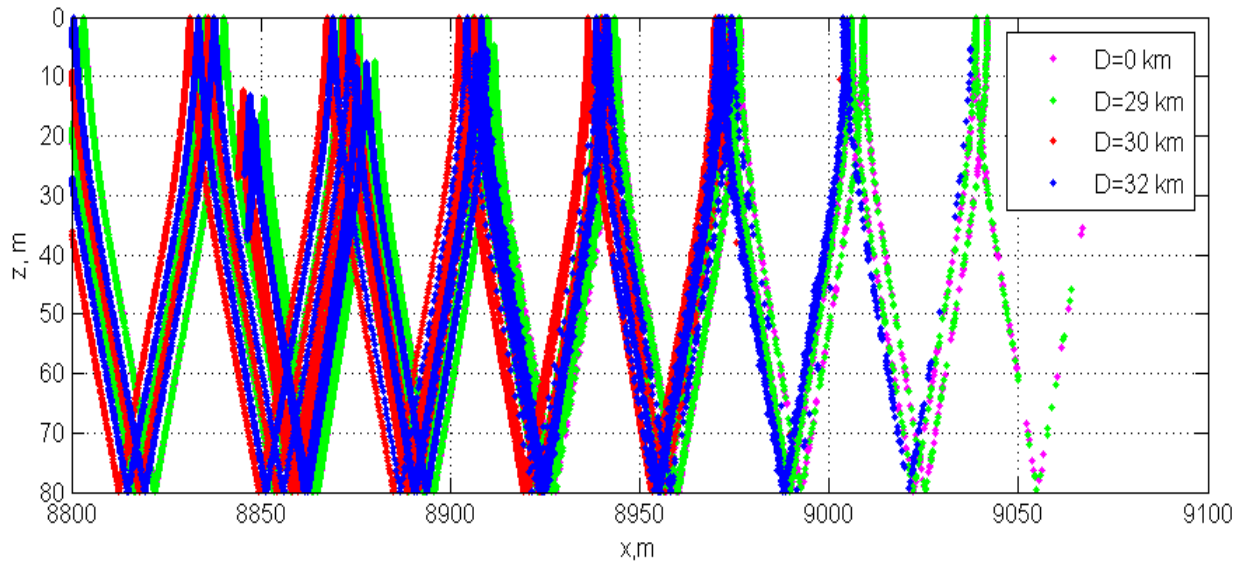


Figure 1. Evolution of an acoustic wavefront during propagation of a packet of nonlinear internal waves. Cross section by the vertical plane $y = 5$ km of the acoustic wavefront at travel time $t = 6$ s is shown for five different stages of the internal wave packet development. A point sound source is located at $(0, 5000 \text{ m}, 20 \text{ m})$. The internal wave train originates at a location with horizontal coordinates $x = 5 \text{ km}, y = 35 \text{ km}$. The packet occupies a circle with radius $D = 0, 29 \text{ km}, 30 \text{ km},$ or 32 km . When $D = 0$, sound propagation is unaffected by internal waves. When $D = 30 \text{ km}$, the maximum of the sound speed perturbations reaches the $y = 5 \text{ km}$ plane.

[The acoustic wavefront consists of a number of connected branches, most of which span the entire waveguide from the seafloor to the ocean surface. The wavefront maintains its general shape during IW packet propagation. It acquires additional branches and extends to larger x values for smaller D values.]

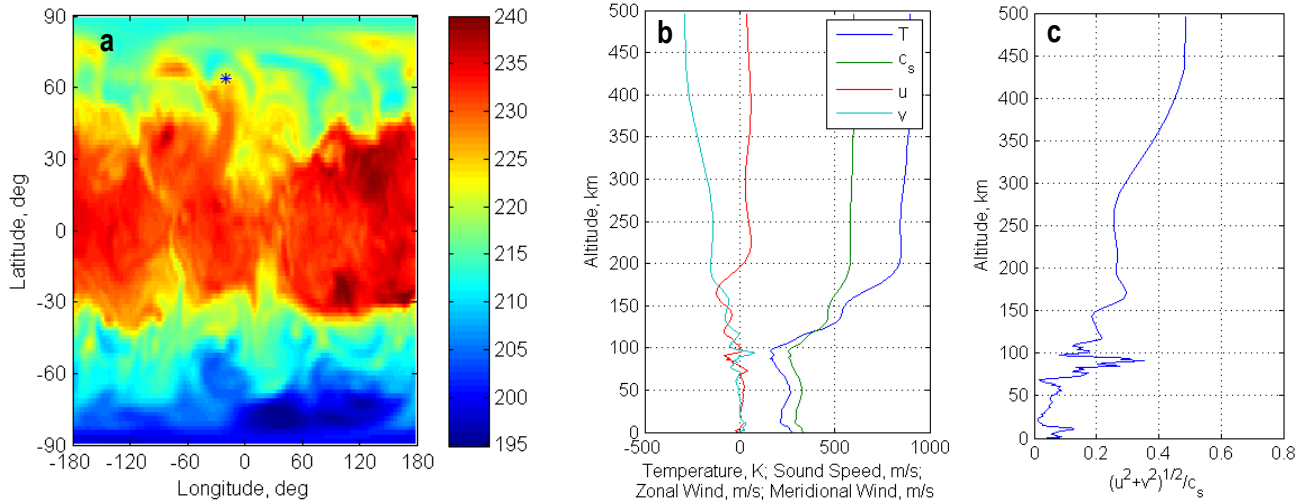


Figure 2. Atmospheric model used in simulations of infrasound propagation. (a) Global distribution of the absolute air temperature (in Kelvin) at altitude 10 km predicted by the Whole Atmosphere Community Climate Model (WAM). Eyjafjallajökull, Iceland, location is marked with an asterisk. (b) Vertical profiles of the temperature T , sound speed c , zonal u and meridional v components of wind velocity at the volcano location. (c) Vertical profiles of the Mach number of wind at the volcano location.

[Globally, absolute air temperature varies between 195 K and 240 K, with the coldest regions between 75 and 90 degrees southern latitude and the hottest regions at 15–35 degrees of southern and northern latitudes in the eastern hemisphere. Above the volcano, the temperature and sound speed vary rapidly below 100 km and steadily increase with height above 100 km. Magnitudes of the zonal and meridional components of the wind velocity reach 130 m/s and 290 m/s, respectively. The maximum value of the Mach number of the wind is about 0.3 below 250 km and 0.5 between 250 and 500 km.]

In acoustic simulations, we disregarded topographic effects and curvature of the Earth and modeled ocean and ground surface as a horizontal plane. With the origin of coordinates chosen at sea level at the location of the Eyjafjallajökull, horizontal coordinate axes Ox and Oy were directed towards east and north, respectively. Although not resolved on the scale of the figures, almost all ray paths in Figure 3a and wavefronts in Figures 3b and 3c are duplicated because of the reflection from the ground in the vicinity of the elevated sound source. Most of the other peculiarities of the ray and wavefront geometry are due to irregular three-dimensional wind distribution predicted by WAM. Note the very strong anisotropy of infrasound propagation in the horizontal plane, which can be appreciated, in particular, from the shape of a wavefront on the ground (Figure 3c).

The critical role of winds in infrasound propagation demands a careful mathematical description of the effects of the fluid flow on acoustic fields. Effective sound speed approximation, where a moving medium is replaced by a motionless fluid with an effective sound speed, is widely used in ocean and atmospheric acoustics. Our HWT algorithm does not rely on the effective sound speed approximation and allows one to quantify its accuracy.

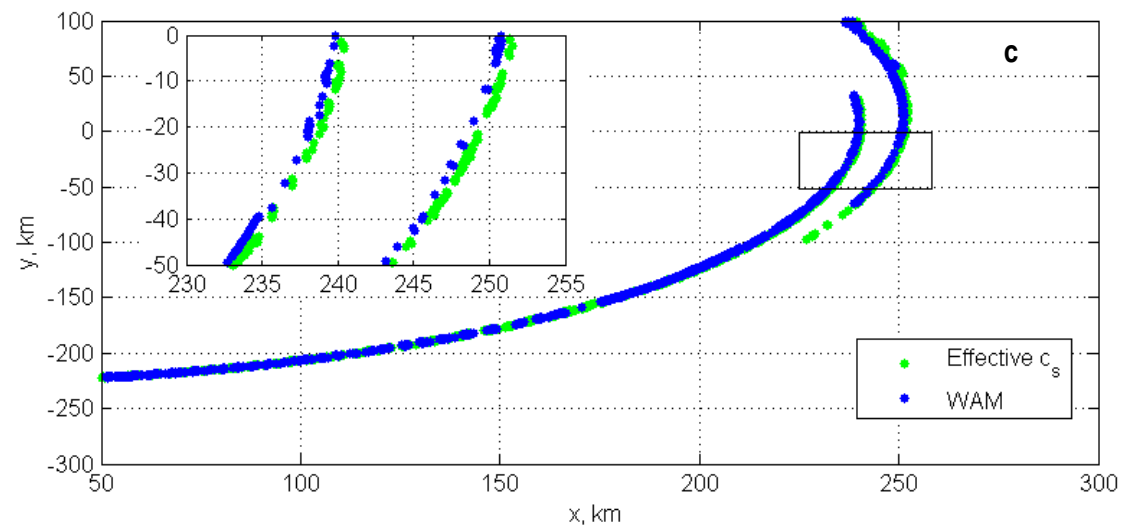
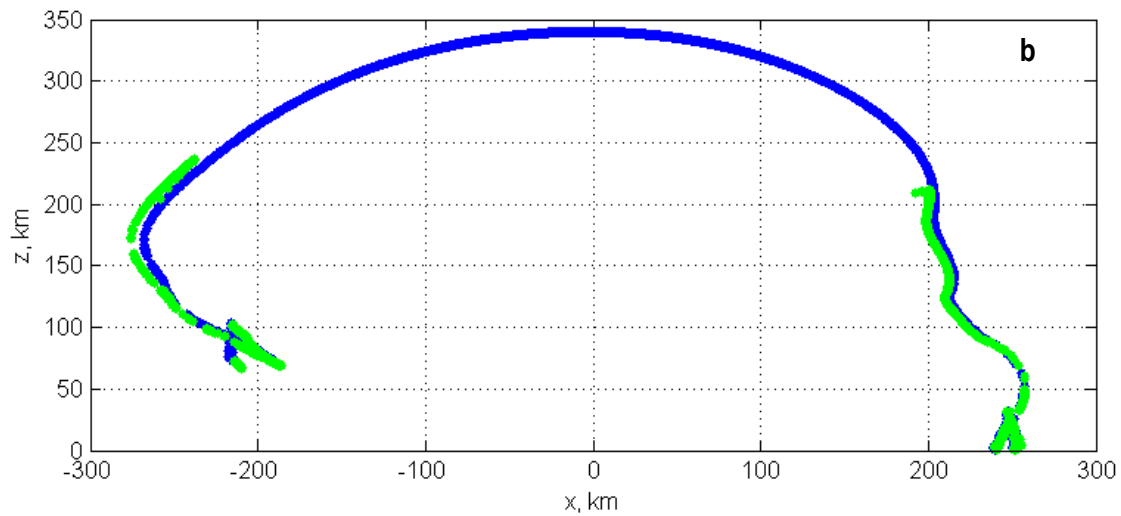
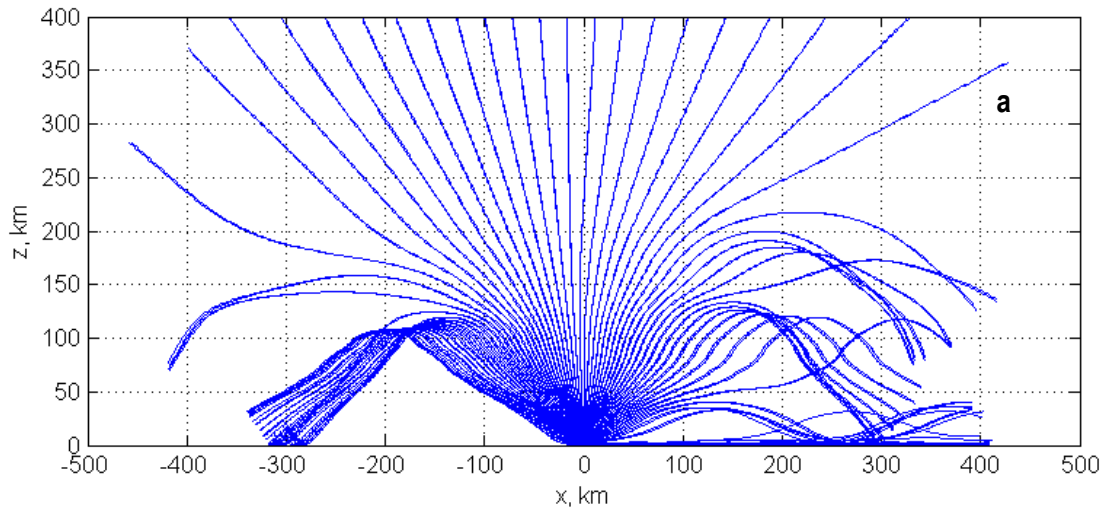


Figure 3. Application of the 3-D HWT algorithm to numerical modeling of infrasound propagation in the atmosphere. (a) Projection on the vertical plane $y = 0$ of rays leaving a point source at the azimuthal angle $\psi = 0$ and with different grazing angles. The point source is placed at the summit of the Eyjafjallajökull volcano at elevation $z_0 = 1666$ m above sea level. (b) Cross section of the acoustic wavefront at $t = 800$ s after an eruption by the vertical plane $y = 0$ passing through the source. In addition to the acoustic wavefront in the atmosphere considered as a moving fluid, the result of calculation of the same wavefront in an “effective” motionless fluid is shown. (c) Intersections of the wavefronts shown in (b) with sea and ground surfaces modeled as the horizontal plane $z = 0$. For comparison of the accurate and approximate wavefront calculations, the insert shows a blow-up of a portion of the wavefronts.

[A projection of a set of rays launched from a point source shows that rays with smaller grazing angles have turning points and can return to the ground to the east and to the west of the source. Turning points occur up to heights as large as 220 km. Steep rays do not have turning points and do not return to the ground. The wavefronts calculated for actual and “effective” motionless fluid become drastically different at high elevations. At ground level, the accurate and approximate calculations give similar results but with ~ 1 km shift between the actual and approximate wavefronts.]

In the Eyjafjallajökull eruption scenario we consider, the most striking differences between wavefronts in moving and “effective” media are observed at large elevations (Figure 3b). Unlike the actual, moving medium, a large shadow zone arises at near-zenith directions in the “effective” medium. The shadow zone leads to termination of the cross section of the approximate wavefront at large heights (Figure 3b). Large distortions of the wavefront position occur at intermediate heights. As expected from theoretical analysis of the effective sound speed approximation accuracy (Godin, 2002), the approximation performs much better for the shallower rays, which are responsible for infrasound arrivals on the ground at $t = 800$ s (Figure 3c). For the portions of the wavefront shown in the insert in Figure 3c, the accurate and approximate wavefronts are separated, on average, by about 1 km, which corresponds to an early arrival bias (i. e., an underestimation of the acoustic travel time) by ~ 3 s in the effective sound speed approximation.

IMPACT/APPLICATIONS

Wavefront tracing has been established as a new approach to modeling sound fields in deep and shallow water, which readily accounts for 3-D propagation effects and current-induced acoustic anisotropy. In addition to modeling acoustic manifestations of internal gravity waves, internal tides, and swell in the ocean, wavefront tracing provides an efficient technique for simulating long-range propagation of infrasound in the atmosphere and infragravity waves in the ocean.

RELATED PROJECTS

None.

REFERENCES

- R. A. Akmaev, Whole atmosphere modeling: Connecting terrestrial and space weather, *Rev. Geophys.* **49**, RG4004 (2011).
- J. R. Apel, A new analytical model for internal solitons in the ocean, *J. Phys. Oceanogr.*, **33**, 2247–2269 (2003)
- J. R. Apel, M. Badiely, C.-S. Chiu, S. Finette, R. Headrick, J. Kemp, J. Lynch, A. Newhall, M. Orr, B. H. Pasewark, D. Tielbuerger, A. Turgutt, K. von der Heydt, and S. Wolf, An overview of the 1995 SWARM shallow-water internal wave acoustic scattering experiment, *IEEE J. Ocean. Eng.*, **22**, 465–500 (1997)
- J. D. Benamou, An introduction to Eulerian geometrical optics (1992-2002), *J. Sci. Computing*, **19**, 63-93 (2003)
- L. M. Brekhovskikh and O. A. Godin, *Acoustics of Layered Media. 2: Point Sources and Bounded Beams*. 2nd edn. (Springer, Berlin etc., 1999)
- K. Chambers and J.-M. Kendall, A practical implementation of wave front construction for 3-D isotropic media, *Geophys. J. Int.*, **174**, 1030–1038 (2008)
- D. P. Drob, M. Garcés, M. Hedlin, and N. Brachet, The temporal morphology of infrasound propagation, *Pure Appl. Geophys.*, **167**, 437–453 (2010)
- O. A. Godin, An effective quiescent medium for sound propagating through an inhomogeneous, moving fluid, *J. Acoust. Soc. Am.*, **112**, 1269–1275 (2002)
- O. A. Godin, Systematic distortions of signal propagation times in random inhomogeneous media, *Doklady Physics*, **48**, 389–394 (2003)
- O. A. Godin, Restless rays, steady wavefronts, *J. Acoust. Soc. Am.*, **122**, 3353–3363 (2007)
- O. A. Godin, Stability of acoustic wave fronts propagating in anisotropic three-dimensional environments, *Acta Acustica united with Acustica*, **95**, 963–974 (2009)
- O. A. Godin, V. U. Zavorotny, A. G. Voronovich, and V. V. Goncharov, Refraction of sound in a horizontally-inhomogeneous, time-dependent ocean, *IEEE J. Oceanic Eng.*, **31**, 384–401 (2006)
- J. Hauser, M. Sambridge, and N. Rawlinson, Multiarrival wavefront tracking and its applications, *Geochem. Geophys. Geosyst.*, **9**, doi:10.1029/2008GC002069 (2008)
- G. Lambaré, P. S. Lucio, and A. Hanyga, Two-dimensional multivalued traveltimes and amplitude maps by uniform sampling of a ray field, *Geophys. J. Int.*, **125**, 584–598 (1996)
- H.-L. Liu, B. T. Foster, M. E. Hagan, J. M. McInerney, A. Maute, L. Qian, A. D. Richmond, R. G. Roble, S. C. Solomon, R. R. Garcia, D. Kinnison, D. R. Marsh, A. K. Smith, J. Richter, F. Sassi, and J. Oberheide, Thermosphere extension of the Whole Atmosphere Community Climate Model, *J. Geophys. Res.* **115**, A12302 (2010)
- P. Sava and S. Fomel, 3-D traveltimes computation using Huygens wavefront tracing, *Geophysics*, **66**, 883–889 (2001)
- J. A. Sethian, Evolution, implementation, and application of level set and fast marching methods for advancing fronts, *J. Comput. Phys.*, **169**, 503-555 (2001)

- J. E. Vidale, Finite-difference calculation of traveltimes in three dimensions, *Geophysics*, **55**, 521–526 (1990)
- V. Vinje, K. Åstebøl, E. Iversen, and H. Gjøystdal, 3-D ray modeling by wavefront construction in open models, *Geophysics*, **64**, 1912–1919 (1999)
- V. Vinje, E. Iversen, and H. Gjøystdal, Traveltime and amplitude estimation using wavefront construction, *Geophysics*, **58**, 1157–1166 (1993)
- N. A. Zabotin, O. A. Godin, P. C. Sava, and L. Y. Zabolina, Acoustic wavefront tracing in inhomogeneous, moving media, *J. Comput. Acoust.*, **20**, Art. 125009 (2012).

PUBLICATIONS

- O. A. Godin, N. A. Zabolina, A. F. Sheehan, and J. A. Collins, Interferometry of infragravity waves off New Zealand, *J. Geophys. Res. Oceans*, **118**, 1103–1122 (2014) [published, refereed]
- N. A. Zabolina, O. A. Godin, P. C. Sava, and L. Y. Zabolina, Tracing three-dimensional acoustic wavefronts in inhomogeneous, moving media, *J. Comput. Acoust.*, **22**, Art. 1450002 (2014) [published, refereed]